CRITICAL INSIGHT

Shedding Light on the Frontier of Photodissociation

Jennifer S. Brodbelt

Department of Chemistry and Biochemistry, University of Texas, Austin, TX 78712, USA

Abstract

The development of new ion activation/dissociation methods is motivated by the need for more versatile ways to characterize structures of ions, especially in the growing arena of biological mass spectrometry in which better tools for determining sequences, modifications, interactions, and conformations of biopolymers are essential. Although most agree that collision-induced dissociation (CID) remains the gold standard for ion activation/dissociation, recent inroads in electron- and photon-based activation methods have cemented their role as outstanding alternatives. This article will focus on the impact of photodissociation, including its strengths and drawbacks as an analytical tool, and its potential for further development in the next decade. Moreover, the discussion will emphasize photodissociation in quadrupole ion traps, because that platform has been used for one of the greatest arrays of new applications over the past decade.

Key words: Photodissociation, Ion activation, Peptide, Tandem mass spectrometry, Ion trap

The field of ion activation/dissociation remains incredibly vibrant due to the ongoing quest to improve the sequencing of biopolymers and map their modifications, to increase the sensitivity to small structural differences, to enhance the ability to differentiate isomers, to facilitate high-throughput applications, and to advance the understanding of fragmentation mechanisms for better automated spectral interpretation. CID has proven to be enormously robust and readily implemented, but insufficient energy deposition and/ or low efficiency for certain fragmentation pathways has stimulated the hunt for other options. There have been several reviews and insightful discussions of electron-based activation methods [1–6], including electron-capture dissociation (ECD) and electron-transfer dissociation (ETD), so these methods will not be extensively addressed in the present article. Examples of some of the more recent photodissociation studies are cited herein, but the citations are by no means comprehensive.

Photodissociation describes the process in which ions are exposed to photons of a selected wavelength, resulting in an accumulation of internal energy that leads to dissociation [7–10]. The activation process may entail the absorption of one or more high-energy UV or visible photons (~2–10 eV/

photon) or tens/hundreds of lower energy IR photons (ca. 0.1 eV/photon). Both pulsed and continuous-wave lasers have been used for photodissociation. The energization period may range from nanoseconds to hundreds of milliseconds based on the photon flux of the laser, the competition between ion activation and collisional cooling, and the energy deposition per photon. The ability to vary photon flux, the total irradiation period, and the selected wavelength endows photodissociation with a high degree of tunability. In fact, it is precisely this type of tunability and the increasing availability of wavelength-tunable lasers coupled to ion trapping mass spectrometers, including Fourier transform ion cyclotron resonance (FTICR) mass spectrometers and quadrupole ion trap systems, that has spurred the fast-growing field of ion spectroscopy (e.g. photodissociation action spectroscopy). Ion spectroscopy entails monitoring the dissociation of mass-selected ions as a function of laser wavelength, yielding a rich vibrational fingerprint. Ion spectroscopy has been the subject of several recent reviews, and will not be discussed further [11–13].

The energization processes in photoactivation is quite different from collisional activation in the sense that the absorption of each photon imparts a discrete amount of energy, unlike the potential range of internal energy deposition upon collisions. Infrared multiphoton dissociation (IRMPD) requires the absorption of multiple low-energy

Correspondence to: Jennifer S. Brodbelt; *e-mail:* jbrodbelt@mail.utexas.edu

photons, making it similar to low-energy CID as a slow heating process. In contrast, the absorption of UV photons leads to the excitation of ions to higher electronic states and access to high-energy dissociation pathways not observed for CID or IRMPD. Photodissociation has been implemented in MALDI time-of-flight mass spectrometers for the analysis of singly charged ions [14–23] and ESI ion trapping instruments (both FTICR systems [24–27] and various quadrupole ion traps [28–63]) for the characterization of singly or multiply charged species. In general, time-of-flight instruments offer the advantages of high resolution, high accuracy, broad m/z range, and fast scan times, although photodissociation efficiencies in these mass spectrometers have been rather low due to the fact that irradiation of the ions occurs orthogonally in a very narrow time window as the selected ions exit the ion gating region. Mainly UV lasers have been utilized for photodissociation on time-of-flight systems due to the need for fast energy deposition. FTICR instruments offer unsurpassed resolution and accuracy and are a natural fit for photon-based activation methods due to their ultra-low pressure environment, which decreases the opportunity for collisional deactivation. Currently the only commercially available instruments equipped with photodissociation capabilities are FTICR mass spectrometers (IRMPD capabilities).

Photodissociation has been successfully implemented on both three dimensional and linear quadrupole ion trap systems. The ability to trap ions is a notable advantage that allows greater flexibility with the choice of laser (pulsed or cw), wavelength (low- or high-energy photons), and activation conditions (single or multiple photons). Moreover, low RF trapping voltages that allow the storage of very low m/z product ions are compatible with the implementation of photoactivation methods. Another characteristic inherent to photon-based activation is the ability to simultaneously energize and dissociate both precursor ions and primary product ions in the trap upon exposure to photons, unlike most collisional activation methods in which only the mass-selected precursor ion, not the resulting product ions, are energized. The conversion of primary product ions to other product ions, a process often termed consecutive dissociation, affords a greater potential array of diagnostic product ions as well as greater spectral complexity. Greater spectral complexity may be viewed as a disadvantage if it subdivides the product ion current into an overly elaborate array of low-abundance products or if the products are small, uninformative ions (like alkyl ions), or it may alternatively be viewed as an advantage by generating a more diverse series of product ions suitable for database search algorithms. Likewise, uninformative "dead-end" product ions, such as those arising from dehydration, may be converted into more informative ions upon consecutive photodissociation.

The concept of coupling lasers to mass spectrometers for photodissociation was demonstrated over three decades ago [64], but the breadth and scope of applications have expanded significantly in the past decade for several reasons.

First, lasers have become more affordable, with cw CO_2 lasers in the range of \$10,000 and UV lasers in the range of \$20,000 and upwards. Second, there has been growing appreciation for the need for alternative ion activation methods, especially with the greater emphasis on solving biological problems. Photon-based activation provides a new avenue for exploration in the context of sequencing biopolymers and pinpointing sites of modifications. Third, photoactivation offers the potential for a high degree of selectivity, not necessarily for bond-specific cleavages but for the selective activation of molecules depending on their available chromophores [27, 40, 42]. This type of selectivity has only rarely been observed for collisional or electron-based activation methods [65–68]. In fact, this selectivity can be viewed alternatively as an advantage (i.e., chromophore-specific activation of molecules) or as a drawback in the sense that the laser wavelength must be matched to chromophores in the targeted molecules to ensure efficient photoabsorption and dissociation. For instance, it is well known that few biomolecules readily absorb 355 nm photons, thus making the third harmonic of a Nd:YAG laser a poor choice for the dissociation of nonderivatized peptides, proteins, nucleic acids, or oligosaccharides. However, tagging these molecules with a suitable chromophore at 355 nm endows them with high absorptivity and allows the potential for facile differentiation and tracking of chromophore-tagged and untagged molecules [47]. A specific example of this strategy will be discussed later [47].

With respect to the nuts and bolts of implementing photodissociation, a mass spectrometer must be equipped with an optical set-up and a means to introduce the photons, typically via an optical window or fiber optic [69]. A method of triggering or gating the laser in a reproducible fashion, as well as timing the irradiation period to coincide with the ions' trajectories through the instrument (for time-of-flight systems) or with the desired ion activation period (for trapping instruments), are other key aspects. Photodissociation can yield informative results even when using fixed-wavelength lasers, such as an economical cw CO_2 laser or a specific excimer laser (e.g., an ArF laser with 193 nm photons), with some tunability in energy deposition based on modulation of the laser power or irradiation time.

A variety of lasers have been used for photodissociation, including CO_2 lasers (10.6 μm, 0.12 eV per photon) [24–27, 40–46, 48–52, 54–56, 61–63], F_2 excimer lasers (157 nm, 7.9 eV per photon) [14–23, 39], ArF excimers (193 nm, 6.4 eV per photon) [57–59], Nd:YAG lasers (266 nm, 4.7 eV per photon [28–32], or 355 nm, 3.5 eV per photon [47, 49]), femtosecond titanium sapphire lasers (800 nm, 1.5 eV per photon) [60], and OPO-Nd:YAG lasers that offer a tunable range from 205 nm to 2550 nm (6.0–0.49 eV per photon) [33–37]. As long as the laser provides sufficient power and offers a wavelength that will be absorbed by the analyte ions of interest, then it can be utilized for photodissociation. Pulsed lasers with low repetition rates (such as 10 Hz or 20 Hz) can be problematic if multiple pulses are

required for efficient photodissociation, leading to low spectral acquisition rates. This is a particular impediment for application on a chromatographic time-scale in which one would prefer an acquisition time of no longer than 100 ms per spectrum to allow adequate signal averaging and chromatographic peak profiling. Focusing the laser offers one way to increase the photon flux through the ion region and enhance the probability of photoabsorption and ion dissociation [61].

The number and types of product ions formed upon photodissociation depends on the wavelength used, and in fact often results in striking differences in the fragmentation patterns from those observed upon CID. Several representative examples are shown in Figures 1 to 3 to illustrate this

point. Figure 1 shows the CID, IRMPD, and UVPD mass spectra obtained for the doubly protonated peptide RPPGFSPFR. Although it is well known that CID typically results in the formation of complementary b and y ions that are useful for peptide sequencing, in the case of RPPGFSPFR the CID spectrum is dominated by ammonia loss and a y_8 ion (a proline-directed cleavage). The corresponding IRMPD spectrum displays a far greater array of product ions, still mostly b and y ions that provide substantially greater sequence coverage. Several immonium ions and internal ions are also formed upon IRMPD. The formation of a larger array of product ions by IRMPD than by CID is attributed to consecutive dissociation of primary product ions upon ongoing photoabsorption, a phenonomen
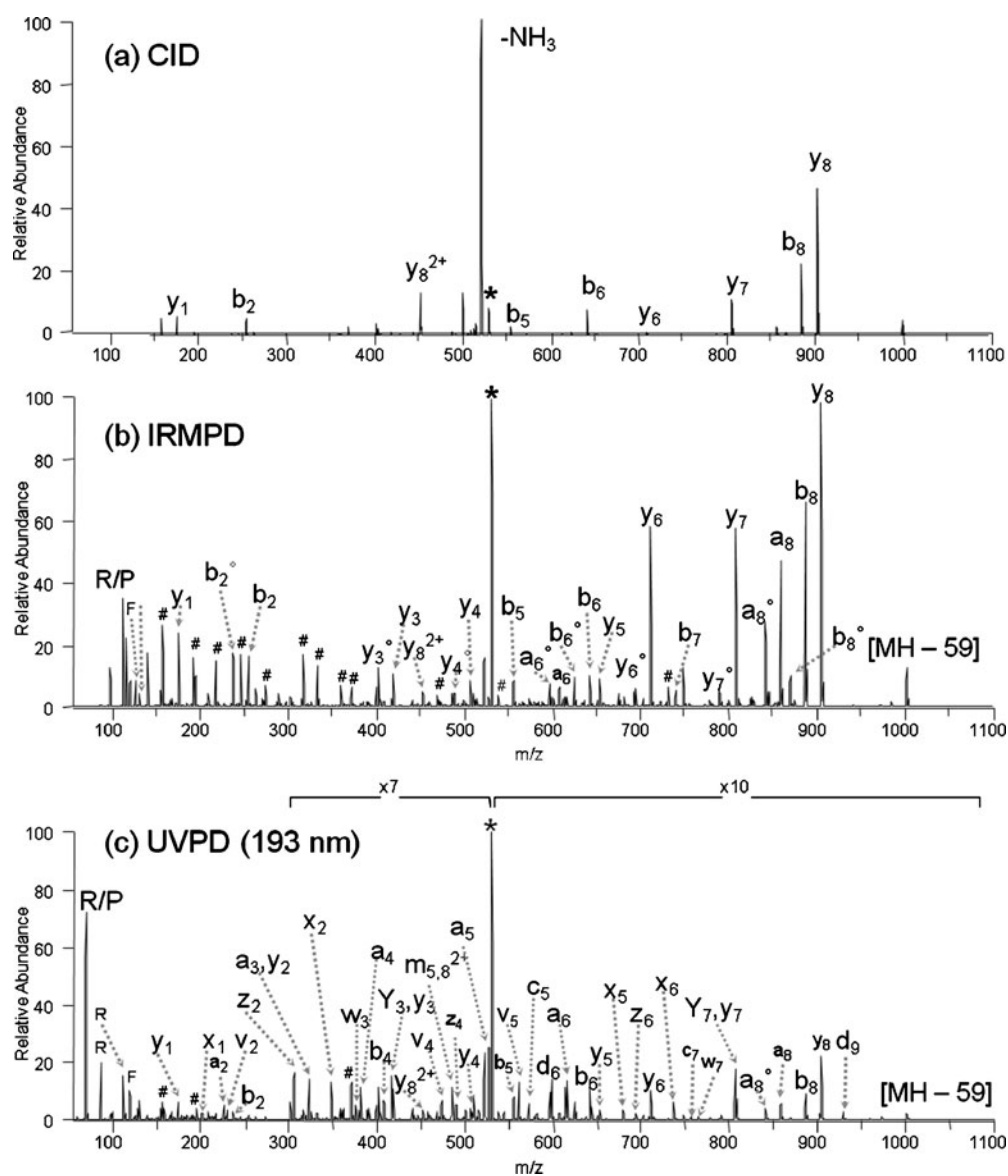

Figure 1. Comparison of the fragmentation patterns obtained for the doubly protonated peptide RPPGFSPFR (*m/z* 530.7) upon (**a**) CID (30 ms, q=0.25, 19% NCE), (**b**) IRMPD (17.5 ms, q=0.09), and (**c**) UVPD (one 5 ns pulse at 193 nm) in a linear ion-trap mass spectrometer. An *asterisk* is used to signify the precursor ion. Internal ions are labeled with the *hash symbol*, #, and ions with an additional loss of water or ammonia are labeled with a *superscript o*
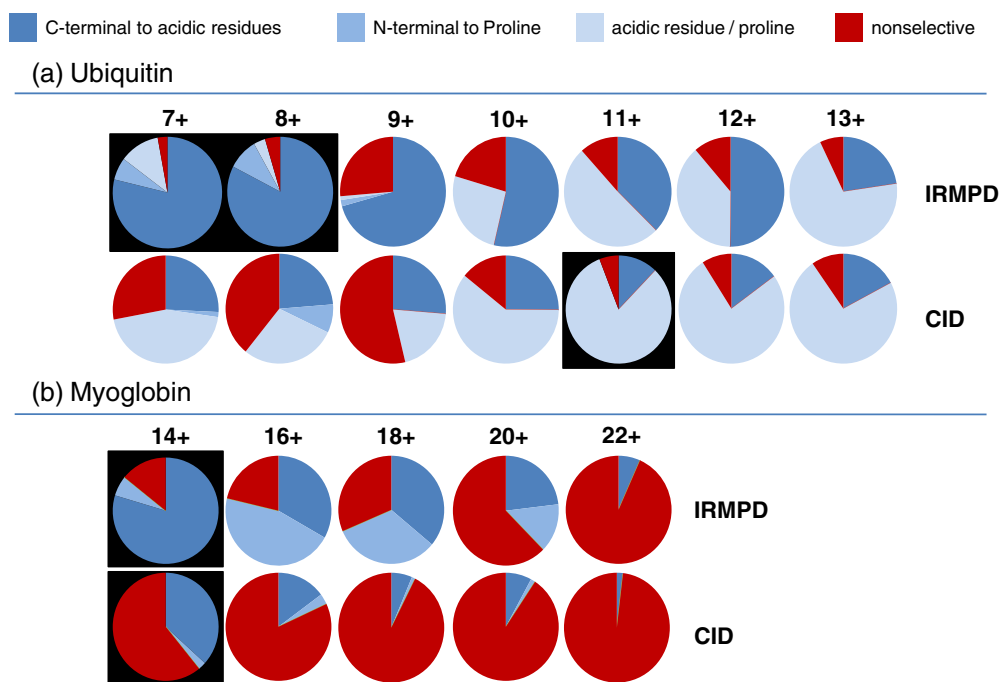
Figure 2. Backbone cleavage site comparison of IRMPD versus CID for (**a**) ubiquitin and (**b**) myoglobin. The *blue-shaded areas* represent the portion of product ions that stem from backbone cleavages that occur C-terminal to acidic residues and/or N-terminal to proline residues. Those product ions that arise from cleavages between DP or EP residues may be classified as both N-terminal to proline and C-terminal to acidic residues, and thus are collectively categorized as "acidic residue/proline" ions (*lightest blue color*). The *red areas* represent the portion of products arising from other nonselective backbone cleavages. The *black boxes* highlight those charge states that dissociated by IRMPD or CID with the highest overall selectivity towards backbone cleavages that occur C-terminal to acidic residues and/or N-terminal to proline. Republished with permission from Madsen, J.A., Gardner, M.W., Smith, S.I., Ledvina, A.R., Coon, J.J., Schwartz, J.C., Stafford, G.C., Brodbelt, J.S.: Top-down protein fragmentation by infrared multiphoton dissociation in a dual pressure linear ion trap. *Anal. Chem*. **81**, 8677–8686 (2009)

arising from the non-mass-selective nature of photoactivation. By using a focused laser or by undertaking IRMPD in a lower pressure ion trap (such as demonstrated in the lower pressure cell of a dual ion-trap mass spectrometer [54]), very high photodissociation efficiencies are possible in less than 15 ms. This makes the feasibility and analytical capabilities of IRMPD on par or better than CID for many applications. Moreover, even very low *m/z* product ions can be observed upon IRMPD, ones that might fall below the trapping range of conventional CID in a quadrupole ion-trap mass spectrometer. Interestingly, the majority of product ions observed upon IRMPD occur as singly charged ions, even from precursor ions that are multicharged. Multicharged product ions undergo efficient consecutive photodissociation, converting them into smaller singly charged products that facilitates their assignment and MS/MS spectral interpretation [52, 54].

IRMPD has also been used successfully for structural characterization of intact proteins (up to 29 kDa) in the low-pressure cell of a dual-cell linear ion trap, thus affording another tool for top-down proteomics applications [55]. In this particular study, consecutive dissociation during IRMPD played a significant role, leading to product ions in substantially lower charge states compared to the product charge states observed upon CID [55]. This outcome

resulted in more accurate mass identification of product ions and facilitated their assignment. IRMPD also provided greater cleavage selectivity than CID, which is a potential benefit for a priori spectral predictions and enhanced database searching for protein identification. Comparisons of the distribution of product ions formed upon IRMPD and CID of multiprotonated ubiquitin and myoglobin are shown in Figure 2 in terms of cleavages that are N-terminal to proline and C-terminal to acidic residues versus those arising from nonselective backbone cleavages (i.e., all other backbone cleavages that lead to other a, b and y ions). The portion of products stemming from selective cleavages are represented by various shades of blue, and nonselective backbone cleavages are by indicated by red. The black highlighted boxes around the pie graphs are used to showcase those charge states that yield the greatest portion of selective backbone cleavages (i.e., largest blue segments), either for IRMPD or CID [55]. IRMPD resulted in an enhancement of backbone cleavages N-terminal to proline and C-terminal to acidic residues compared to CID. This trend was most apparent for the lowest precursor charge states, making this fragmentation selectivity even more predictable.

IRMPD has also proven effective for the structural characterization of many classes of molecules, ranging from
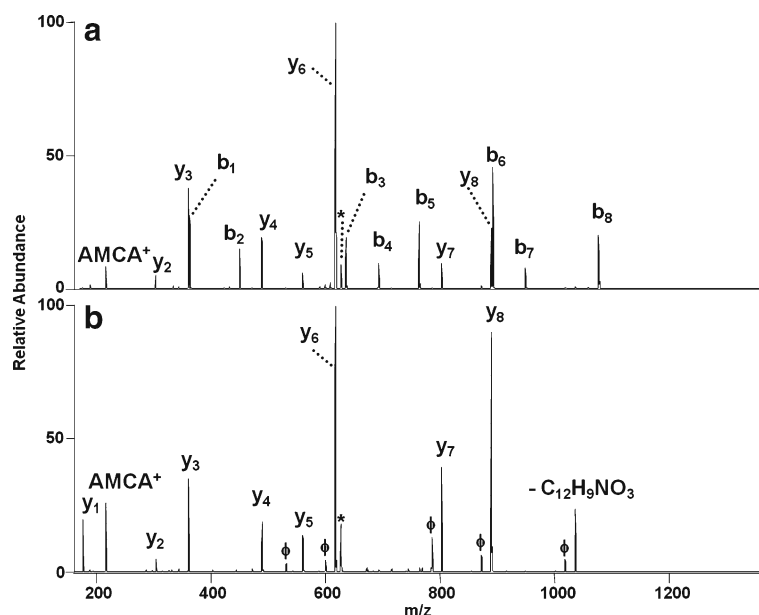
Figure 3. ESI-MS/MS spectra of the doubly protonated N-terminally modified AMCA-modified peptide FSWGAEGQR by (**a**) CID (0.50 V) and (**b**) UVPD (15 pulses at 10 Hz). UVPD shows a complete series of y ions with minimal complexity due to the elimination of the redundant b ions. The peak with the $-C_{12}H_9NO_3$ label corresponds to the loss of the charged AMCA moiety from the N-terminus of the peptide, thus producing the unmodified, singly charged peptide species. An *asterisk* is used to signify the precursor ion. The *φ symbol* indicates ammonia losses from the adjacent y ions. Republished from Wilson, J., Brodbelt, J.S.: MS/MS simplification by 355 nm ultraviolet photodissociation of chromophore-derivatized peptides in a quadrupole ion trap. *Anal. Chem.* **79**, 7883–7892 (2007)

peptides and proteins, as described above, to small organic molecules like drugs and natural products, as well as oligosaccharides [48] and nucleic acids [41, 45, 46]. Nucleic acids have some of the highest photoabsorptivities and corresponding IR photodissociation efficiencies of any class of molecules. The phosphate backbone promotes high IR absorptivity at 10.6 μm, resulting in high-energy deposition with irradiation times as low as a few milliseconds. The IRMPD spectra display a tremendous array of sequence ions (namely a – B and w ions for oligodeoxyribonucleotides and c- and y-type ions for oligoribonucleotides).

One positive attribute of IRMPD is that it can be classified a generally universal activation method, as nearly all molecules display some degree of absorptivity in the IR range, including the wavelength of the common CO_2 laser (10.6 μm). On the downside, each IR photon only contains a small amount of energy (e.g., 0.12 eV at 10.6 μm), meaning that numerous photons must be absorbed for sufficient energy accumulation to cause dissociation. Absorption of multiple photons requires longer activation times with competition from collisional cooling or radiative relaxation [61, 63]. To mitigate the latter problems, focusing the laser increases the photon density through the ion region and accelerates the rate of energy accumulation [61]. Alternatively, higher-energy deposition is possible by elevating the temperature of the bath gas (a process termed "thermally assisted IRMPD") [63], or by using photons with shorter wavelengths.

For example, one of the newest photodissociation methods employed a near-IR Ti-sapphire femtosecond laser (800 nm wavelength, 1.5 eV per photon) [60]. The resulting spectra for peptides contained a rich array of sequence ions, including a, b, c, x, y, and z ions.

Absorption of UV photons leads to even higher internal energy deposition (ranging from 3.5 to 7.9 eV per photon for typical UV lasers) than occurs upon the absorption of an IR photon. However, absorption of UV photons is a more selective process, meaning that only those ions with suitable UV chromophores will absorb. Nonetheless, there have been significant inroads in the application of UVPD, with recent studies aimed at the analysis of nucleic acids, peptides, and oligosaccharides [14–19, 28–39, 47, 49, 53, 58–60].

For example, activation of multiply charged peptide cations upon the absorption of 193 nm photons produces a mixture of a, b, c, x, y, and z ions and a few lower abundance w and v side-chain loss ions, as well as some immonium ions, as illustrated in the UVPD spectrum shown in Figure 1c along with the companion CID spectrum for comparison [58]. The diverse array of N- and C-terminal ions makes the UVPD spectra well adapted for in silico database algorithms that typically search multiple product ion types simultaneously. Photodissociation efficiencies range from 50 to 98% using a single 5 ns laser pulse, making the method amenable to high-throughput proteomic strategies. Interestingly (but not completely unexpectedly), it

has been found that peptides with one or more amino acids containing aromatic side chains yield higher dissociation efficiencies than peptides without aromatic groups, thus showing the impact of suitable UV chromophores on photoabsorptivity. There has been a flurry of recent reports demonstrating the analytical utility of UVPD for increasingly impressive biological applications [16, 19], such as the identification of peptides derived from ribosomal proteins [70] and from lysed human HT-1080 cytosolic fibrosarcoma cells [58]. UVPD has compared favorably to CID for the identification of peptides, an outcome attributed to the higher information content of the UVPD spectra, which contained diagnostic a, b, c, x, y, z product ions, often with full sequence coverage from both series of N-terminal and C-terminal ions, and v and w side-chain loss ions that allow the differentiation of isobaric amino acids. In some cases, UVPD has even allowed the identification of more peptides and yielded higher searching scores than CID. Moreover, the UV activation method proved faster, requiring only a single 5 ns, 8 mJ laser pulse, making it attractive for high-throughput, shotgun-style proteomic strategies.

Even in the absence of natural chromophores, molecules can be derivatized to attach chromophores and endow them with high photoabsorptivity at specific wavelengths. There have been several recent studies demonstrating this concept, either to enhance the photoabsorption/photodissociation efficiencies of classes of molecules or to incorporate unique photoabsorptivity to promote selective photodissociation for targeted applications [44, 47–51, 53, 59]. For example, peptides do not contain natural chromophores at 355 nm; therefore, they would not be expected to absorb nor dissociate upon exposure to 355 nm photons [47]. However, the attachment of specific UV chromophores allows the efficient photoactivation of not only the precursor ions but also any products that retain the chromophore functionality. In the example shown in Figure 3, the FSWGAEGQR peptide was modified at its N-terminus by attaching 7-amino-4-methyl coumarin-3-acetic acid succinimidyl ester (AMCA), which contains a strong UV chromophore. CID of this derivatized peptide led to the conventional series of b and y ions [47]. The complexity of the corresponding UVPD spectrum was simplified substantially, resulting in a single series of y ions that proved amenable to de novo interpretation. De novo methods derive the amino acid sequence information from the observed spectrum based on knowledge of the peptide fragmentation pattern [71]. Because database searching methods identify only a fraction of the peptides from their MS/MS spectra, de novo strategies could supplement peptide sequencing, especially for the interpretation of peptide sequences from unknown proteins or ones with modifications. As illustrated in Figure 3, the AMCA-modified peptide yielded a complete series of y ions down to the y_1 ion, facilitating the confident sequencing of this peptide [47]. The lack of b ions in the UVPD spectra

arose directly from their high photoabsorptivity due to the incorporation of the chromophore at the N-terminus—the b ions undergo rapid and efficient consecutive fragmentation upon exposure to additional photons, ultimately leading to their near-complete annihilation from the spectra. This is a case in which derivatization of the analyte molecules altered their absorptivities and conferred a high degree of activation specificity.

A different type of selectivity can be promoted by conjugating a chromophore to targeted groups of molecules in the presence of other nontargeted molecules in mixtures, facilitating rapid differentiation of the groups of molecules. For example, an IR-absorbing phosphate functional group was incorporated into a protein crosslinking agent (shown in the inset of Figure 4a), affording selective IRMPD of only the crosslinked peptides in a mixture containing many other peptide species (mostly uninformative noncrosslinked peptides) [50]. Endowing only the crosslinked peptides with special IR absorptivity allowed them to be selectively tracked in a very complex mixture of peptides, thus addressing one of the key challenges of utilizing mass spectrometry for protein crosslinking studies in which the structural information from just a few low-abundance species must be extracted from an enormously complicated soup of peptides. The IR-chromogenic crosslinker was used to explore the conformation of ubiquitin by forming crosslinks between proximate lysine residues, followed by the tryptic digestion of the crosslinked ubiquitin and then LCMS analysis [50]. The eluting species were transmitted into an ion trap and then irradiated with IR photons in alternative scans. Only the peptides containing the IR-absorbing crosslinker responded and underwent IRMPD upon exposure to 50 ms of 10.6 μm radiation (Figure 4a), allowing them to be rapidly and confidently differentiated from noncrosslinked products. Moreover, the IRMPD mass spectra of the crosslinked peptides displayed a series of b- and y-type ions (Figure 4b) that allowed successful sequencing and identification of four sites of conjugation without the need for collision induced dissociation. For example, IRMPD of the crosslinked peptide that eluted around 37.5 minutes resulted in an array of diagnostic sequence ions (Figure 4b). All of the y ions C-terminal to the two crosslinked lysine residues were detected using IRMPD, and three $b_{n\beta}$ product ions were detected, providing confirmation of the identity of the β peptide, $L^{43}IFAGIK^{48}QLEDGR^{54}$. The net crosslinked product consisted of $T^{55}LSDYNIQK^{63}ESTLHLVLR^{72}$ (α peptide) linked to $L^{43}IFAGK^{48}QLEDGR^{54}$ (β peptide) through Lys-63 and Lys-48, spanning a distance of 18.4Å in ubiquitin.

There have been several other recent reports of characteristic fragmentation pathways observed upon UVPD, typically catalyzed by the presence of specific functional groups or modified residues [20, 28, 29, 31, 37]. In one study, abundant $a_n − 97$ product ions were detected at each phosphorylated residue upon the UVPD (193 nm) of protonated phosphopeptides containing a basic amino acid
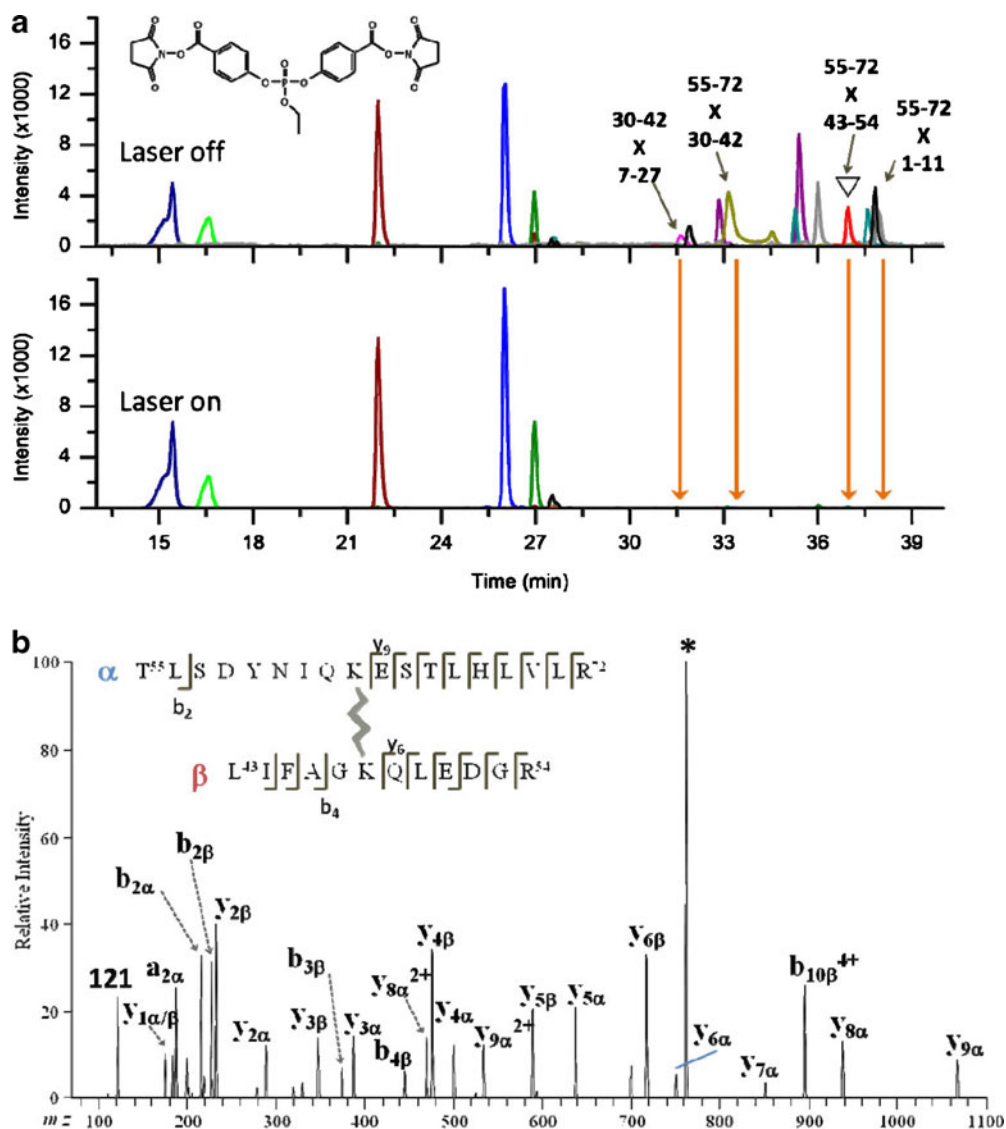
Figure 4. (a) Reconstructed ion chromatograms of isolation (50 ms) and IRMPD (50 ms, 50 W) spectra of a tryptic digest of ubiquitin crosslinked by IRCX. The identities of the products are labeled based on the crosslinked residues. (b) IRMPD spectrum (30 ms, 50 W, q = 0.1) of tryptic peptide of ubiquitin crosslinked by IRCX acquired during data-dependent LC-IRMPD-MS of [T^{55}LSDYNIQK^{63}ESTLHLVLR^{72} Ä IRCX Ä L^{43}IFAGIK^{48}QLEDGR^{54} + 5H]$^{5+}$, m/z 762.4 which is the crosslinked peptide labeled with the triangle in (a). The first peptide listed is the α peptide; the second peptide is referred to as the β peptide. Lysine residues in bold font indicate the site of the crosslink. An asterisk (*) is used to signify the precursor ion. Republished from Gardner, M., Vasicek, L., Shabbir, S., Anslyn, E., Brodbelt, J.S.: Chromogenic crosslinker for the characterization of protein structure by infrared multiphoton dissociation mass spectrometry. *Anal. Chem.* **80**, 4807–4819 (2008)

at the N-terminus [20]. In another investigation, a specific C$_\alpha$–C$_\beta$ bond cleavage was reported for protonated tyrosine-containing peptides upon UVPD at 262 nm, resulting in a radical product ion in which a specific portion of the tyrosyl residue was cleaved [37]. UV activation (266 nm) has also been reported to induce site-specific reactions at iodo-derivatized tyrosines [28, 29, 31], as demonstrated for an array of peptides and cytochrome c. Photoactivated iodine loss by homolytic bond cleavage resulted in the formation of radical products that subsequently underwent selective

collision-induced cleavage near the original iodo-labeled tyrosines. In another study, selective homolytic cleavage of a C–S bond associated with a quinone-modified cysteine side chain and the formation of site-specific d ions occurred upon 266 nm photoexcitation of 1,4-naphthoquinone-derivatized peptides and proteins [29]. These recent examples illustrate the potential for more inspiring applications that manipulate the selectivity promoted by photoactivation.

Another attribute of photodissociation arises from the ease with which photodissociation can be integrated with

other activation methods, thus creating hybrid activation strategies that offer exciting possibilities for addressing some of the most challenging structural characterization problems. For example, photodissociation can be united with CID or electron-based activation techniques to allow even more flexibility for manipulating energy deposition, to create more selective activation sequences, and ultimately to yield more specific information about ion structures, sequences, and modifications [33, 36, 72]. We have recently begun to integrate collision-, electron-, and photon-based activation methods to explore their utility for pinpointing very specific and/or subtle structural features of modified biological molecules, such as peptides or nucleic acids. As an example, cisplatin is a well-characterized nucleic acid interactive agent, binding covalently to GG, GNG, or AG, mostly by intrastrand crosslinks. CID of the resulting oligonucleotide/cisplatin complex resulted in relatively few backbone cleavages (Figure 5a). A hybrid activation strategy was implemented in which a precursor ion of interest was subjected to an electron-transfer reaction, resulting in a charge-reduced product which was subsequently characterized by IRMPD [72]. The hybrid ET-IRMPD spectrum differs significantly in the overall distribution of product ions (Figure 5b), with also a significant increase in the number of diagnostic cleavages along the backbone. The emergence of a, d, and z ions, along with the w and a − B ions, allows unambiguous characterization of the GG

cisplatin binding site. In general, the hybrid MS/MS techniques result in a more diverse array of product ions than any single activation method alone.

Outlook

Photodissociation offers compelling advantages as an activation method, including access to high-energy, tunable, and generally well-defined energy deposition. The use of photons instead of collisions alleviates any potential ion-scattering effects and obviates the need to introduce a collision gas. Both precursor ions and product ions may undergo photoactivation and dissociation, leading to a greater range of product ions that may provide a more specific structural fingerprint or may be useful for database search and de novo algorithms. The characteristics of ion dissociation are largely dependent on the wavelength used for photoactivation, in some cases leading to a more diverse array of fragmentation pathways and in other cases resulting in dissociation very similar to conventional CID. The opportunity to develop strategies that exploit the selectivity of photoexcitation, either based on the incorporation of chromophores that convert non-absorbing molecules into absorbing molecules or by enhancing site-specific or bond-selective cleavages, is a fascinating frontier for photodissociation.
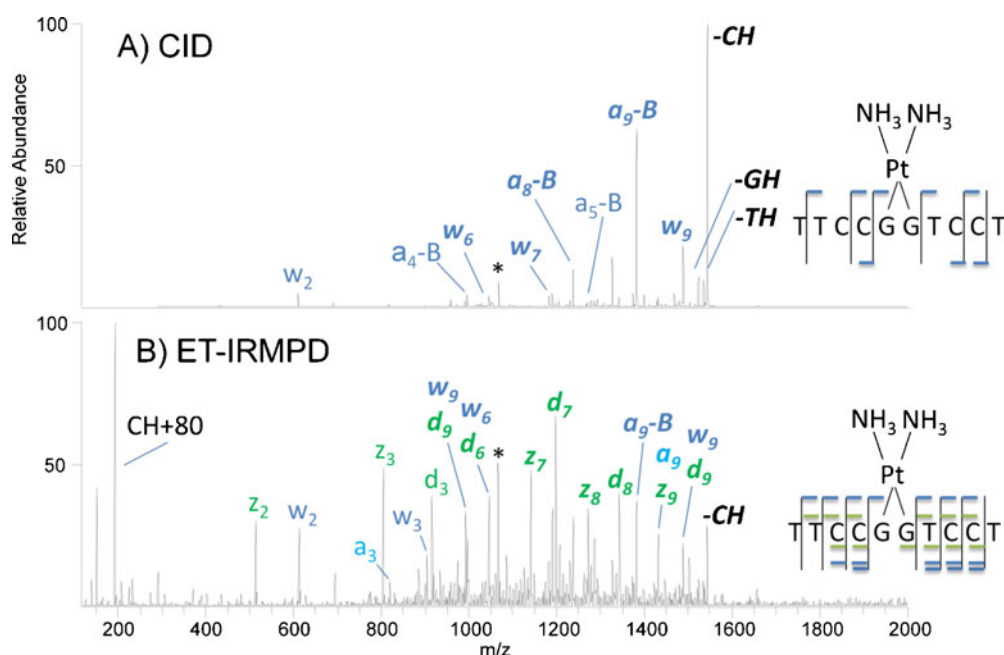

Figure 5. Comparison of (**a**) CID (3+ charge state, 10% normalized collision energy) and (**b**) hybrid ET-IRMPD (ET-IRMPD, electron-transfer reactions of 4+ charge state, followed by IRMPD of the resulting 3+• ion for 4 ms at 10 W) of the cisplatin adduct of oligodeoxynucleotide TTCCGGTCCT in a linear ion-trap mass spectrometer. The ions labeled in *bold italics* contain the cisplatin adduct. The sequence diagrams shown in the *insets* indicate the range of diagnostic ions detected. An *asterisk* is used to signify the precursor ion. Republished from Smith, S.I., Brodbelt, J.S., Hybrid Activation Methods for Elucidating Nucleic Acid Modifications, *Anal. Chem.* **81** (2011) in press

The promising allure of photodissociation does not come without some drawbacks. The expense of a laser is an unavoidable upfront cost, although significantly less than the mass spectrometer itself or many of its most common auxiliary components, such as an HPLC system. Most of the more affordable lasers are not tunable, meaning that there is limited flexibility for exploring the significant array of photodissociation strategies with a single laser. To date, photodissociation has only been offered as an option on one type of commercial mass spectrometer (an FTICR system). The main factors that likely have limited more widespread adaptation for other commercial mass spectrometers include concerns about laser safety, the need for robust laser alignment with the ion region for optimal performance (with the expectation that the typical user does not have significant laser and optics expertise), and concerns about the cost of the laser relative to conventional CID. None of these issues is insurmountable, and many anticipate the greater adoption of photodissociation as an option in future generations of commercial mass spectrometers, especially given the impressive applications of photodissociation that have emerged in recent years.

Acknowledgments

References

1. Zubarev, R.: Electron capture dissociation and other ion-electron fragmentation reactions. In: Laskin, J., Lifshitz, C. (Eds.): Principles of Mass Spectrometry Applied to Biomolecules. Wiley: Hoboken, 475–517 (2006)
2. Bakhtiar, R., Guan, Z.: Electron capture dissociation mass spectrometry in characterization of peptides and proteins. *Biotechnol. Lett.* **28**, 1047–1059 (2006)
3. Zubarev, R.A., Zubarev, A.R., Savitski, M.M.: Electron capture/transfer versus collisionally activated dissociations: solo or duet? *J. Am. Soc. Mass Spectrom.* **19**, 753–761 (2008)
4. Mikesh, L.M., Ueberheide, B., Chi, A., Coon, J.J., Syka, J.E.P., Shabanowitz, J., Hunt, D.F.: The utility of ETD mass spectrometry in proteomic analysis. *Biochim. Biophys. Acta* **1764**, 1811–1822 (2006)
5. Wiesner, J., Premsler, T., Sickmann, A.: Application of electron transfer dissociation (ETD) for the analysis of post-translational modifications. *Proteomics* **8**, 4466–4483 (2008)
6. Coon, J.J.: Collisions or electrons? Protein sequence analysis in the 21st century. *Anal. Chem.* **81**, 3208–3215 (2009)
7. Brodbelt, J.S., Wilson, J.J.: Infrared multiphoton dissociation in quadrupole ion traps. *Mass Spectrom. Rev.* **28**, 390–424 (2009)
8. Ly, T., Julian, R.R.: Ultraviolet photodissociation: developments towards applications for mass-spectrometry-based proteomics. *Angew. Chem. Int. Ed.* **48**, 7130–7137 (2009)
9. Reilly, J.T.: Ultraviolet photofragmentation of biomolecular ions. *Mass Spectrom. Rev.* **28**, 425–447 (2009)
10. Dunbar, R.C.: Photodissociation of biomolecule ions: progress, possibilities, and perspectives coming from small-ion models. In: Laskin, J., Lifshitz, C. (Eds.): Principles of Mass Spectrometry Applied to Biomolecules. Wiley: Hoboken, NJ, 337–377 (2006)
11. Baer, T., Dunbar, R.C.: Ion spectroscopy: where did it come from; where is it now; and where is it going? *J. Am. Soc. Mass Spectrom.* **21**, 681–693 (2010)
12. Polfer, N.C., Oomens, J.: Vibrational spectroscopy of bare and solvated ionic complexes of biological relevance. *Mass Spectrom. Rev.* **28**, 468–494 (2009)
13. Eyler, J.R.: Infrared multiple photon dissociation spectroscopy of ions in Penning traps. *Mass Spectrom. Rev.* **28**, 448–467 (2009)
14. Thompson, M.S., Cui, W., Reilly, J.P.: Fragmentation of singly charged peptide ions by photodissociation at 157 nm. *Angew. Chem. Int. Ed.* **43**, 4791–4794 (2004)
15. Cui, W., Thompson, M.S., Reilly, J.P.: Pathways of peptide ion fragmentation induced by vacuum ultraviolet light. *J. Am. Soc. Mass Spectrom.* **16**, 1384–1398 (2005)
16. Zhang, L., Reilly, J.P.: Peptide de novo sequencing using 157 nm photodissociation in a tandem time-of-flight mass spectrometer. *Anal. Chem.* **82**, 898–908 (2010)
17. Kim, T.-Y., Reilly, J.P.: Time-resolved observation of product ions generated by 157 nm photodissociation of singly protonated phospho-peptides. *J. Am. Soc. Mass Spectrom.* **20**, 2334–2341 (2009)
18. Thompson, M.S., Cui, W., Reilly, J.P.: Factors that impact the vacuum ultraviolet photofragmentation of peptide ions. *J. Am. Soc. Mass Spectrom.* **18**, 1439–1452 (2007)
19. Parthasarathi, R., He, Y., Reilly, J.P.: New insights into the vacuum UV photodissociation of peptides. *J. Am. Chem. Soc.* **132**, 1606–1610 (2010)
20. Shin, Y.S., Moon, J.H., Kim, M.S.: Observation of phosphorylation site-specific dissociation of singly protonated phosphopeptides. *J. Am. Soc. Mass Spectrom.* **21**, 53–59 (2010)
21. Yoon, S.H., Moon, J.H., Kim, M.S.: Dissociation mechanisms and implication for the presence of multiple conformations for peptide ions with arginine at the C-terminus: time-resolved photodissociation study. *J. Mass Spectrom.* **45**, 806–814 (2010)
22. Moon, J.H., Yoon, S.H., Bae, Y.J., Kim, M.S.: Dissociation kinetics of singly protonated leucine enkephalin investigated by time-resolved photodissociation tandem mass spectrometry. *J. Am. Soc. Mass Spectrom.* **21**, 1151–1158 (2010)
23. Shin, Y.S., Moon, J.H., Kim, M.S.: Construction and performance test of a multiplex multistage (MSn) time-of-flight mass spectrometer. *Anal. Chem.* **80**, 9700–9704 (2008)
24. Dodds, E.D., German, J.B., Lebrilla, C.B.: Enabling MALDI-FTICR-MS/MS for high-performance proteomics through combination of infrared and collisional activation. *Anal. Chem.* **79**, 9547–9556 (2007)
25. Bindila, L., Steiner, K., Schaeffer, C., Messner, P., Mormann, M., Peter-Katalinic, J.: Sequencing of O-glycopeptides derived from an S-layer glycoprotein of *Geobacillus stearothermophilus* NRS 2004/3a containing up to 51 monosaccharide residues at a single glycosylation site by Fourier transform ion cyclotron resonance infrared multiphoton dissociation mass spectrometry. *Anal. Chem.* **79**, 3271–3279 (2007)
26. McFarland, M.A., Marshall, A.G., Hendrickson, C.L., Nilsson, C.L., Fredman, P., Mansson, J.E.: Structural characterization of the GM1 ganglioside by infrared multiphoton dissociation, electron capture dissociation, and electron detachment dissociation electrospray ionization FT-ICR MS/MS. *J. Am. Soc. Mass Spectrom.* **16**, 752–762 (2005)
27. Flora, J.W., Muddiman, D.C.: Determination of the relative energies of activation for the dissociation of aromatic versus aliphatic phosphopep-tides by ESI-FTICR-MS and IRMPD. *J. Am. Soc. Mass Spectrom.* **15**, 121–127 (2004)
28. Ly, T., Julian, R.R.: Elucidating the tertiary structure of protein ions in vacuo with site specific photoinitiated radical reactions. *J. Am. Chem. Soc.* **132**, 8602–8609 (2010)
29. Diedrich, J.K., Julian, R.R.: Site-selective fragmentation of peptides and proteins at quinine-modified cysteine residues investigated by ESI-MS. *Anal. Chem.* **82**, 4006–4014 (2010)
30. Sun, Q., Yin, S., Loo, J.A., Julian, R.R.: Radical directed dissociation for facile identification of iodotyrosine residues using electrospray ionization mass spectrometry. *Anal. Chem.* **82**, 3826–3833 (2010)
31. Liu, Z., Julian, R.R.: Deciphering the peptide iodination code: influence on subsequent gas-phase radical generation using photodissociation ESI-MS. *J. Am. Soc. Mass Spectrom.* **20**, 965–971 (2009)
32. Ly, T., Julian, R.R.: Residue-specific radical-directed dissociation of whole proteins in the gas phase. *J. Am. Chem. Soc.* **130**, 351–358 (2008)
33. Larraillet, V., Antoine, R., Dugourd, P., Lemoine, J.: Activated-electron photodetachment dissociation for the structural characterization of protein polyanions. *Anal. Chem.* **81**, 8410–8416 (2009)
34. Racaud, A., Antoine, R., Joly, L., Mesplet, N., Dugourd, P., Lemoine, J.: Wavelength-tunable ultraviolet photodissociation (UVPD) of hep-

arin-derivated disaccharides in a linear ion trap. *J. Am. Soc. Mass Spectrom.* **20**, 1645–1651 (2009)

35. Tabarin, T., Antoine, R., Broyer, M., Dugourd, P.: Specific photodissociation of peptides with multi-stage mass spectrometry. *Rapid Commun. Mass Spectrom.* **19**, 2883–2892 (2005)

36. Gabelica, V., Tabarin, T., Antoine, R., Rosu, F., Compagnon, I., Broyer, M., De Pauw, E., Dugourd, P.: Electron photodetachment dissociation of DNA polyanions in a quadrupole ion trap mass spectrometer. *Anal. Chem.* **78**, 6564–6572 (2006)

37. Joly, L., Antoine, R., Broyer, M., Dugourd, P., Lemoine, J.: Specific UV photodissociation of tyrosyl-containing peptides in multistage mass spectrometry. *J. Mass Spectrom.* **42**, 818–824 (2007)

38. Larraillet, V., Vorobyev, A., Brunet, C., Lemoine, J., Tsybin, Y.O., Antoine, R., Dugourd, P.: Comparative dissociation of peptide polyanions by electron impact and photo-induced electron detachment. *J. Am. Soc. Mass Spectrom.* **21**, 670–680 (2010)

39. Kim, T.Y., Thompson, M.S., Reilly, J.P.: Peptide photodissociation at 157 nm in a linear ion trap mass spectrometer. Rapid Commun. *Mass Spectrom.* **19**, 1657–1665 (2005)

40. Crowe, M., Brodbelt, J.S.: Infrared multiphoton dissociation (IRMPD) and collisionally activated dissociation of peptides in a quadrupole ion trap with selective IRMPD of phosphopeptides. *J. Am. Soc. Mass Spectrom.* **15**, 1581–1592 (2004)

41. Keller, K.M., Brodbelt, J.S.: Collisionally activated dissociation and infrared multiphoton dissociation of oligonucleotides in a quadrupole ion trap. *Anal. Biochem.* **326**, 200–210 (2004)

42. Crowe, M.C., Brodbelt, J.S.: Differentiation of phosphorylated and unphosphorylated peptides by high-performance liquid chromatography/electrospray ionization/infrared multiphoton dissociation in a quadrupole ion trap. *Anal. Chem.* **77**, 5726–5734 (2005)

43. Wilson, J.J., Brodbelt, J.S.: Infrared multiphoton dissociation for enhanced de novo sequence interpretation of N-terminal sulfonated peptides in a quadrupole ion trap. *Anal. Chem.* **78**, 6855–6862 (2006)

44. Pikulski, M., Wilson, J., Aguilar, A., Brodbelt, J.S.: Amplification of infrared multiphoton dissociation efficiency in a quadruple ion trap by using IR-active ligands. *Anal. Chem.* **78**, 8512–8517 (2006)

45. Wilson, J., Brodbelt, J.S.: Infrared multiphoton dissociation of duplex DNA/drug complexes in a quadrupole ion trap. *Anal. Chem.* **79**, 2067–2077 (2007)

46. Mazzitelli, C.L., Brodbelt, J.S.: Probing ligand binding to duplex DNA using $KMnO_4$ reactions and electrospray ionization tandem mass spectrometry. *Anal. Chem.* **79**, 4636–4647 (2007)

47. Wilson, J., Brodbelt, J.S.: MS/MS simplification by 355 nm ultraviolet photodissociation of chromophore-derivatized peptides in a quadrupole ion trap. *Anal. Chem.* **79**, 7883–7892 (2007)

48. Pikulski, M., Hargrove, A., Shabbir, S., Anslyn, E., Brodbelt, J.S.: Sequencing and characterization of oligosaccharides using infrared multiphoton dissociation and boronic acid derivatization in a quadrupole ion trap. *J. Am. Soc. Mass Spectrom.* **18**, 2094–2106 (2007)

49. Wilson, J., Brodbelt, J.S.: Ultraviolet photodissociation at 355 nm of fluorescently-labeled oligosaccharides. *Anal. Chem.* **80**, 5186–5196 (2008)

50. Gardner, M., Vasicek, L., Shabbir, S., Anslyn, E., Brodbelt, J.S.: Chromogenic crosslinker for the characterization of protein structure by infrared multiphoton dissociation mass spectrometry. *Anal. Chem.* **80**, 4807–4819 (2008)

51. Vasicek, L.A., Wilson, J.J., Brodbelt, J.S.: Improved infrared multiphoton dissociation of peptides through N-terminal phosphonite derivatization. *J. Am. Soc. Mass Spectrom.* **20**, 377–384 (2009)

52. Madsen, J.A., Brodbelt, J.S.: Comparison of infrared multiphoton and collision induced dissociation of supercharged peptides in ion traps. *J. Am. Soc. Mass Spectrom.* **20**, 349–358 (2009)

53. Gardner, M.W., Brodbelt, J.S.: Ultraviolet photodissociation mass spectrometry of bis-aryl hydrazone conjugated peptides. *Anal. Chem.* **81**, 4864–4872 (2009)

54. Gardner, M.A., Ledvina, A.R., Smith, S., Madsen, J., Schwartz, G.C., Stafford, G.C., Coon, J.J., Brodbelt, J.S.: Infrared multiphoton dissociation of peptide cations in a dual quadrupole linear ion trap mass spectrometer. *Anal. Chem.* **81**, 8109–8118 (2009)

55. Madsen, J.A., Gardner, M.W., Smith, S.I., Ledvina, A.R., Coon, J.J., Schwartz, J.C., Stafford, G.C., Brodbelt, J.S.: Top-down protein fragmentation by infrared multiphoton dissociation in a dual pressure linear ion trap. *Anal. Chem.* **81**, 8677–8686 (2009)

56. Gardner, M.W., Li, N., Ellington, A.D., Brodbelt, J.S.: Infrared multiphoton dissociation of small-interfering RNA anions and cations. *J. Am. Soc. Mass Spectrom.* **21**, 580–591 (2010)

57. Smith, S.I., Brodbelt, J.S.: Characterization of oligodeoxynucleotides and modifications by 193 nm photodissociation and electron photodetachment. *Anal. Chem.* **82**, 7218–7226 (2010)

58. Madsen, J., Boutz, D., Brodbelt, J.S.: Ultrafast ultraviolet photodissociation at 193 nm and its applicability to proteomic workflows. *J. Proteome Research* **9**, 4205–4214 (2010)

59. Vasicek, L., Brodbelt, J.S.: Enhancement of ultraviolet photodissociation efficiencies through attachment of aromatic chromophores. *Anal. Chem.* (2010). Accepted

60. Kalcic, C.L., Gunaratne, T.C., Jones, A.D., Dantus, M., Reid, G.E.: Femtosecond laser-induced ionization/dissociation of protonated peptides. *J. Am. Chem. Soc.* **131**, 940–942 (2009)

61. Newsome, G.A., Glish, G.L.: Improving IRMPD in a quadrupole ion trap. *J. Am. Soc. Mass Spectrom.* **20**, 1127–1131 (2009)

62. Remes, P.M., Glish, G.L.: Mapping the distribution of ion positions as a function of quadrupole ion trap mass spectrometer operating parameters to optimize infrared multiphoton dissociation. *J. Phys. Chem. A* **113**, 3447–3454 (2009)

63. Payne, A.H., Glish, G.L.: Thermally assisted infrared multiphoton photodissociation in a quadrupole ion trap. *Anal. Chem.* **73**, 3542–3548 (2001)

64. Woodin, R.R., Bomse, D.S., Beauchamp, J.L.: Multiphoton dissociation of gas-phase ions using low intensity cw radiation. In: Moore, C.B. (Ed.): Chemical and Biochemical Applications of Lasers, Vol. IV. Academic: New York, 355–388 (1979)

65. Gardner, M., Brodbelt, J.S.: Preferential cleavage of N–N hydrazone bonds for sequencing bis-arylhydrazone conjugated peptides by electron transfer dissociation. *Anal. Chem.* **82**, 5751–5759 (2010)

66. Chowdhury, S.M., Munske, G.R., Tang, X., Bruce, J.E.: Collisionally activated dissociation and electron capture dissociation of several mass spectrometry-identifiable chemical cross-linkers. *Anal. Chem.* **78**, 8183–8193 (2006)

67. Soderblom, E.J., Goshe, M.B.: Collision-induced dissociative chemical cross-linking reagents and methodology: applications to protein structural characterization using tandem mass spectrometry analysis. *Anal. Chem.* **78**, 8059–8068 (2006)

68. Lu, Y., Tanasova, M., Borhan, B., Reid, G.E.: Ionic reagent for controlling the gas-phase fragmentation reactions of cross-linked peptides. *Anal. Chem.* **80**, 9279–9287 (2008)

69. Drader, J.J., Hannis, J.C., Hoftstadler, S.A.: Infrared multiphoton dissociation with a hollow fiber waveguide. *Anal. Chem.* **75**, 3669–3674 (2003)

70. Zhang, L., Reilly, J.P.: De novo sequencing of tryptic peptides derived from deinococcus radiodurans ribosomal proteins using 157 nm photodissociation MALDI TOF/TOF mass spectrometry. *J. Proteome Res.* **9**, 3025–3034 (2010)

71. Seidler, J., Zinn, N., Boehm, M.E., Lehmann, W.D.: De novo sequencing of peptides by MS/MS. *Proteomics* **10**, 634–649 (2010)

72. Smith, S.I., Brodbelt, J.S.: Hybrid activation methods for elucidating nucleic acid modifications. *Anal. Chem.* **81**, (2011) in press